Proceedings of 9th IEEE International Conference
on CYBER Technology in Automation, Control, and Intelligent Systems
July 29- August 2, 2019, Suzhou, China

Mechatronic Design of a Novel Robotic Manta with Pectoral Fins*

Yan Meng, Zhengxing Wu, and Junzhi Yu, *Senior Member, IEEE*

***Abstract*—This paper proposes an innovative design scheme of a manta-inspired robot system for both fast swimming and high maneuverability. Based on some hydrodynamic and biological studies on manta rays, a new pectoral fin with two separate DOFs is designed, to mimic the compound motion of two vertical waves as well as the tip trajectory of the natural pectoral fin, which have important influence on the efficient swimming of manta rays. Besides, a special buoyance adjustment mechanism is incorporated to pursue gliding ability and three-dimensional maneuverability of robotic manta. With novel structural design and powerful servomotors, the robotic manta is expected to achieve high propulsion efficiency while maintaining good swimming speed. Specifically, the motion principles and geometrical parameters of the pectoral fin are discussed in detail. Moreover, the basic control method of robotic manta is given and simulation analyses are conducted to verify the presented new design.**

I. Introduction

As one of the oldest vertebrates in the world, fish has evolved excellent underwater movement systems with high efficiency, low-noise, and high maneuverability in the struggle for survival over hundreds of millions of years. Compared with traditional underwater vehicles driven by propellers, fish has better adaptability to complex environment [1]. These superior characteristics of fish have gathered much attention in both academia and industry over the last two decades. As early as 1994, researchers at MIT developed the first bionic robot fish RoboTuna, which aimed to explore the long endurance and high efficiency propulsion mode of underwater vehicles [2]. Subsequently, some efforts focus on fishlike swimming mechanism, gliding ability, and multi robotic fish coordination were launched [3]. In addition, some mission-oriented researches based on robotic fish platforms, such as underwater exploration and underwater rescue, have also become research hotspots [4].

In nature, the propulsion mode of fish can be roughly divided into two categories: body and/or caudal fin (BCF) mode and median and/or paired fin (MPF) mode. Fish using BCF mode depends on its flexible body and caudal fin to generate the main propulsion, while the other utilizes its median and pectoral fins to realize swimming. Manta rays, the largest of more than 500 species of rays, are typical of MPF swimming mode [5]. With relatively rigid dorsoventrally compressed bodies and expanded pectoral fins, manta rays can forage at a speed of 0.25–0.47m/s when measured by satellite tags, and have high maneuverability as well as excellent gliding ability [6]. Researches on manta ray have been carried out for many years, and can be divided into two categories from the perspective of driving mode. One kind is propelled by motors, such as the RoMan I-III, developed by Nanyang Technology University (NTU), and Robo-Ray I-IV developed by Beihang University [7]. These researches have achieved good results in terms of swimming speed and gliding ability, but are limited by the rigid structure, which results in simplification of the movement of pectoral fins. The other is driven by new materials such as SMA and artificial muscle. For example, the Aqua Ray, developed by Festo, is propelled by fluidic muscle. The Aqua Ray can realize the motion form close to manta rays and has high swimming efficiency [8]. However, the speed and volume of Aqua Ray were limited for lack of driving power. Therefore, it is necessary to develop a robotic manta which possesses both enough swimming speed and complex motion form closed to natural manta rays.

The flapping of large flatten pectoral fins plays a key role in manta's highly efficient swimming. Pectoral fin propulsion can be classified as either undulatory or oscillatory according to the ratio of the wavelength travelling wave to the mean chord length. Manta rays, are typically oscillatory, like some birds. An important characteristic of their locomotion is the generation of a traveling wave along the stream wise chord of pectoral fins, coupled with a vertical wave along the wingspan from the baseline of their bodies [9] [10]. In this paper, a new type of mechanical pectoral fin is presented. With the improved crank rocker mechanism, the robotic manta can flap along the wingspan. In the meantime, the propulsive wave along the stream wise is realized by means of mechanical parallel connection. Other studies have pointed out that the net thrust for propulsion of manta rays is produced from the distal half of the fins. Moreover, the tip trajectory of pectoral fins has an important impact on manta's swimming efficiency [6]. Therefore, on the basis of main flapping and wave movements, a bevel gear mechanism is added to each pectoral fin to acquire a horizontal DOF, which helps to realize the tip trajectory tracking.

The gliding movement of manta rays is an important swimming mode in their long distance voyage. In recent years, researches on various underwater gliders are emerging one after another, such as Commodities-Slocum, Seaglider, and Spray [11]–[13]. Equipped with buoyancy adjustment mechanism which directly regulates the pose, these gliders can achieve floating and diving at the cost of very low energy

*This work was supported by the National Natural Science Foundation of China (nos. 61725305, 61836015, 61633004, and 61633017) and by the Pre-research fund of Equipments of China (61403120108).

Y. Meng and Z. Wu are with the State Key Laboratory of Management and Control for Complex Systems, Institute of Automation, Chinese Academy of Sciences, Beijing 100190, China and University of Chinese Academy of Sciences, Beijing 100049, China. (e-mail: menyan2017@ia.ac.cn, zhengxing.wu@ia.ac.cn).

J. Yu is with the State Key Laboratory of Management and Control for Complex Systems, Institute of Automation, Chinese Academy of Sciences, Beijing 100190, China and the State Key Laboratory for Turbulence and Complex System, Department of Mechanics and Engineering Science, BIC-ESAT, College of Engineering, Peking University, Beijing 100871, China (e-mail: junzhi.yu@ia.ac.cn).

978-1-7281-0770-7/19/$31.00 ©

consumption. Inspired by the above studies, we design buoyancy adjustment mechanism with symmetrical warehouses, which are suitable for the broaden profile of the manta ray and effectively save the internal space of the robotic manta. The buoyancy adjustment mechanism can not only help the robotic manta ray to achieve the gliding movement, but also coordinate with the free movement mode to realize flexible three-dimensional (3D) movements.

The rest of this paper is organized as follows. In Section II, the overall structure design of the robotic manta is presented. Based on the novel mechanical system, Solidworks simulation and locomotion control analysis are offered in Section III. Finally, the conclusion and future work are given in Section IV.

II. Mechatronic Design of the Robotic Manta

With the purpose of realizing the complex motion form of manta rays, a novel robotic manta with unique pectoral fins is conceived. Fig. 1 presents the conceptual model.

The robotic manta is divided into four major parts: a head cabinet equipped with a ZED depth camera, a central cabinet containing a buoyancy adjustment mechanism and control units, two pectoral fins as the main propeller, and a caudal fin for auxiliary adjustment. In order to enhance the waterproof performance, the head and central cabinet are made of ABS material and sealed with waterproof rubber ring. The central cabin is arranged in a stepped layout. Other devices are fixed on the bottom plate, inserted from the front. Note that both the pectoral fins and caudal fin are driven by waterproof servomotors, which are directly exposed to the water for easy adjustment and disassembly. Distinct from the previous researches, the robotic manta employs a pair of pectoral fins with two separate DOFs, which contributes to the realization of compound movement. Based on the biological dynamic model of manta rays [14], the robotic manta is expected to achieve high swimming efficiency. Generally, the robotic manta is 375 mm long and 718 mm wide. TABLE I lists the detailed technical specification of the robotic manta.

Manta rays are known for their fast, efficient, and highly maneuverable swimming. According to some biological studies, the superior swimming performance of manta rays comes from the flapping of the wide pectoral fins which are also the key parts of depth and turning control. With complex 3D motion, two pectoral fins can effectively generate hydrodynamic forces and produce highly efficient propulsion [14]. This is also the focus of this paper.

In order to mimic the complex 3D movement of the pectoral fin of manta rays, two significant aspects are taken into consideration. On the one hand, the basic structure of the pectoral fin is determined according to the superposition motion of flapping and propulsive wave along stream wise. On the other hand, the special tip trajectory of the pectoral fin is tracked by compound motion.

A. Basic Structure of the Pectoral Fin

Biologists identified that the deformation of the pectoral fins due to flapping can be decomposed into waves A and B perpendicular to each other, as illustrated in Fig. 2 [15].

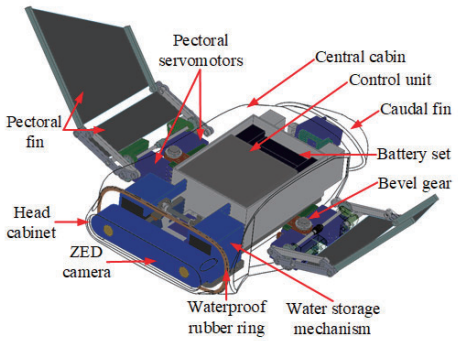

Fig. 1. Illustration of concenptual design of the robotic manta.

TABLE I. Main Technical Specification of the Robotic Manta

Items	Characteristics
Dimension	718 × 375 × 113 mm^3
Control unit	ARM Cortex-M4
Sensors	Pressure sensor, IMU, ZED Camera
Drivers	Servomotors (GDW893MG)
Power	DC 8.4 V

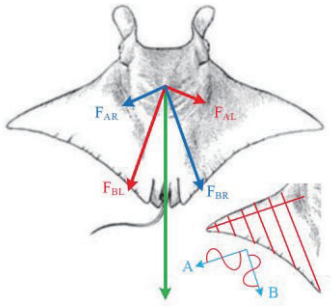

Fig. 2. Propulsion forces generated by wave A and wave B [15].

Among them, wave A produces propulsive forces F_{AL} and F_{AR} along the span wise, while wave B produces propulsive forces F_{BL} and F_{BR} along the stream wise. In particular, manta ray obtains momentum under mutual effect of these forces. When the two pectoral fins move symmetrically, the component forces along the span wise cancel each other out, and the manta ray can move in a straight line. When the movements of two pectoral fins are asymmetrical, the turning movement can be induced.

Based on the four-bar crank rocker mechanism, as illustrated in Fig. 3, a new type of pectoral fin is formed. The linkage group I and II are crank rocker mechanisms of similar structure. Then the torque is generated by the single servomotor of the linkage group I, and transmitted to the linkage group II through the gear set mechanism with a gear tooth coupling. A wide flexible fin film is attached to the two linkage groups and moves with them to generate propulsive force. Fig. 4 (a) describes the movement principle of the linkage group I. Rod *b* is directly connected with the servomotor as input end. Rod *f* (short rod) and *i* (long rod) are connected with the flexible fin film as two output ends. When rod *b* is driven by the servomotor and rotates counterclockwise, rod *f* and rod *i* can generate asynchronous swings share the

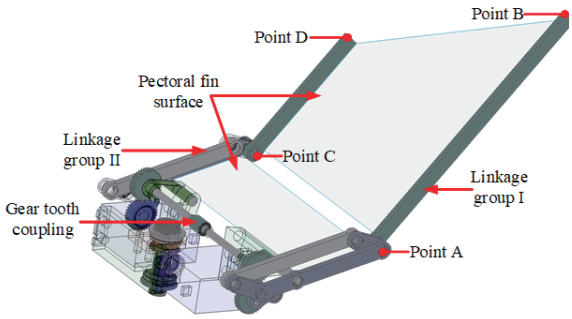

Fig. 3. Structual representation of the single pectoral fin.

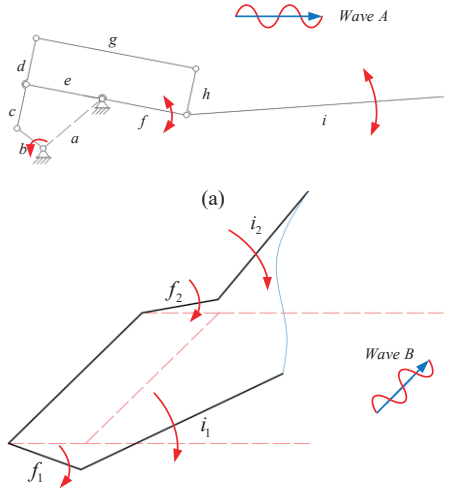

Fig. 4. Demonstration of the waves generated by linkage groups. (a) Wave A; (b) Wave B.

same period. The rod *f and i* go through their up and down strokes respectively, and the movement of rod *f* precedes the rod *i*. The movements of two rods forms wave A in the plane of the linkage group, which generates F_{AL} and F_{AR}.

Further, we denote the drive rod of two linkage groups as b_1 and b_2 respectively. To acquire the propulsive wave along stream wise, we make the two drive rods in different rotation angle by adjusting the gear tooth coupling. Then the two sets of output rods (f_1, f_2, i_1, i_2) run at different phases, as shown in Fig. 4 (b). At a certain down stroke, when the initial angle of rod *b* of the linkage group I leads rod *b* of linkage group II, the swing of the output rods f_1 and i_1 will also lead f_2 and i_2, so that wave B is generated along the stream wise, and the propulsive forces (F_{BL} and F_{BR}) are obtained.

Since all the rods are non-retractable, once their length is determined, the range of the swing angle of the output rods and the phase difference of the periodic motion will also be uniquely determined. Therefore, reasonable selection of rod length is the key to design. For this reason, several typical positions of crank rocker mechanism are analyzed, and the related parameters are formulated.

Fig. 5 shows limit positions of the short rod *f* in up and down strokes. θ_{down}, θ_{up}, φ_{down} and φ_{up} are the acute angles

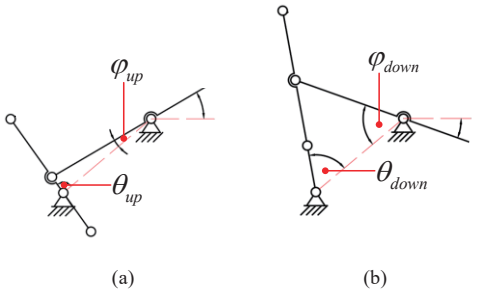

Fig. 5. Two limit positions of the rod *i*. (a) Up limit position; (b) Down limit position.

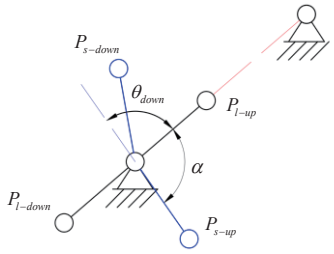

Fig. 6. Four limit positions corresponding to the rod *b*.

between rod *b* and *a* and the acute angles between rod *e* and *a* at two limit positions. According to the triangle relationship, it follows that

$$\begin{cases} \cos\theta_{down} = \dfrac{a^2+(b+c)^2-e^2}{2a(b+c)} \\ \cos\theta_{up} = \dfrac{a^2+(c-b)^2-e^2}{2a(c-b)} \\ \cos\varphi_{down} = \dfrac{a^2+e^2-(b+c)^2}{2ae} \\ \cos\varphi_{up} = \dfrac{a^2+e^2-(c-b)^2}{2ae} \end{cases} \tag{1}$$

It is worth noting that rod *b* driven by the servomotors is the main power component and the key of angle control. As shown in Fig. 6, P_{l-up}, P_{s-up}, P_{l-down} and P_{s-down} represent four special movement positions of rod *b*, corresponding to the limit positions of two output rods respectively. Then the angle ratio of two strokes and the amplitude ($\varphi_{l-\text{flap}}$) of swing of the short rod can be determined during one motion cycle of rod *b*. $\theta_{u-\text{range}}$ and $\theta_{d-\text{range}}$ represent the angular range of rod *b* corresponding to the two stokes of the short rod over one motion cycle. The derived formula is as follows:

$$\begin{cases} \theta_{d-\text{range}} = \pi - \theta_{up} + \theta_{down} \\ \theta_{u-\text{range}} = 2\pi - \theta_{d-\text{range}} = \pi + \theta_{up} - \theta_{down} \\ ratio = \dfrac{\theta_{u-\text{range}}}{\theta_{d-\text{range}}} = \dfrac{\pi+(\theta_{up}-\theta_{down})}{\pi-(\theta_{up}-\theta_{down})} \\ \varphi_{s-\text{flap}} = \varphi_{down} - \varphi_{up} \end{cases} \tag{2}$$

For long rod *i*, the two positions where rod *a* rod *b* are collinear can be regarded as the two limit positions of its

TABLE II. MAIN STUCTRAL PARAMETERS OF THE CRANK ROCKER MECHANISM

Parameters	Value
ratio	0.57 : 0.43
α	90°
$\varphi_{s-\text{flap}}$	50°
$\varphi_{l-\text{flap}}$	90°
a	50 mm
b	20.75 mm
c	29.25 mm
e	50 mm

motion. According to the geometric relationship, the ratio of the angular range of rod *b* corresponding to rod *i* is always 1:1. $\varphi_{l-\text{flap}}$, the relative swing amplitude of rod *i*, can be further determined on the basis of $\varphi_{s-\text{flap}}$.

In addition, the angular difference between P_{s-up} and P_{l-up} can be approximately regarded as the phase difference of two output rods, denoted as α. From the geometric relationship, it is not difficult to derive that

$$\alpha = \pi - \theta_{down}. \tag{3}$$

In order to mimic the motion form of the pectoral fin of natural manta rays, relevant biological data is exploited to determine the concrete sizes. Subsequently, the length of the rods is optimized to avoid interference of the actual mechanical structure. The resulting structural parameters are shown in TABLE II.

B. Tip Trajectory Tracking Mechanism

The above model approximates the basic propulsion mode of manta ray on the basis of simplification. However, the actual movement of the pectoral fin is very complicated due to its soft characteristics. Some studies have revealed that main thrust of manta rays is generated by the distal half of their pectoral fins [6]. Besides, the tip trajectory of the pectoral fin has significant effect on swimming efficiency [16]. As shown in Fig. 7 (a), the tip trajectory forms an irregular closed pattern in three-dimension space when the manta ray swim stably. A horizontal rotation DOF is added to each pectoral fin, so that the fins can achieve motion compound, which help the robotic manta track the tip trajectory. Moreover, the horizontal DOF can be used to adjust the direction of two vertical propulsion forces and is expected to explore more swimming modes of robotic manta.

The detailed structure is shown in Fig. 7 (b). A set of bevel gears is utilized to transmit the torque of servomotor vertically to the entire plane of pectoral fins. Under the condition of narrow installation space, the pectoral fins are allowed to swing in the horizontal plane. Fig. 8 depicts a top view of the horizontal rotation of the pectoral fins. The red and blue trapezoids represent the two limit positions of the horizontal movement, respectively. Considering the physical interference of the actual structure, the theoretical horizontal swing angle can reach 40°, and its swing amplitude reaches 0.4 BL, which satisfies the requirement of trajectory tracking.

C. Buoyancy Adjustment Mechanism

For manta rays and most birds, efficient gliding movement

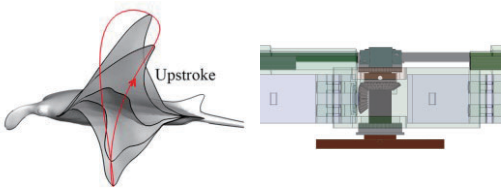

(a) (b)

Fig. 7. (a) Lateral view of the tip trajectory [6]; (b) Demonstration of the bevel gear mechanism.

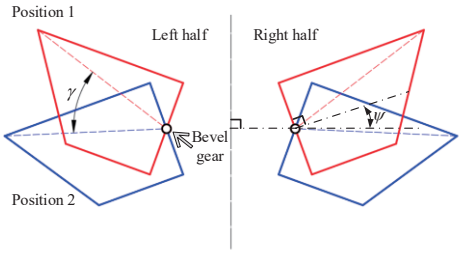

Fig. 8. Top view of the horizontal movement of pectoral fins.

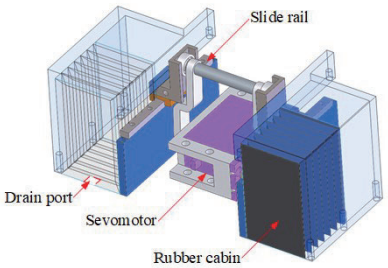

Fig. 9. Conceptual design of the novel buoyancy adjustment mechanism.

is the key to long endurance. Similarly, for the robotic manta, due to its limited internal space, low energy density, mechanical friction and wear, it is difficult to guarantee long duration just relying on the conventional swimming mode. To this end, a new type of buoyancy adjustment mechanism is designed to achieve the gliding movement of the robotic manta. The conceptual model is shown in Fig. 9.

In accordance with the manta ray's broad profile, the entire buoyancy adjustment mechanism consists of two symmetrical parts. When the mechanism is working, the rod driven by servomotor drags the slide block to move on the slide rail so as to change the volume of the rubber cabin. Finally, the water flows in and out through the drain port at the bottom of the rubber cabin. Specifically, the rubber cabin is encased in plastic housing to limit its position, and all components are attached to an aluminum base plate.

In addition, the manta ray's caudal fin also has some influence on attitude adjustment. Therefore, a single servomotor is employed, as shown in Fig. 1, to coordinate the movement of the pectoral fins and the buoyancy adjustment mechanism, expecting to acquire better swimming performance.

III. LOCOMOTION CONTROL

After determining the basic structure of the robotic manta, we further analyze its motion control which is divided into two parts: basic motion and compound motion.

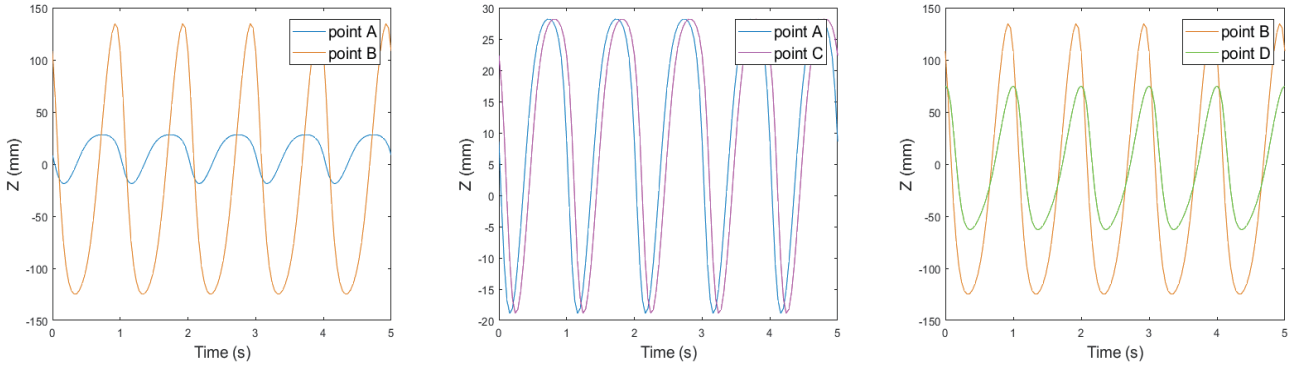

Fig. 10. Vertical displacement of four key points. (a) Point A and point B; (b) Point A and point C; (c) Point B and point D.

A. Basic Motion

The robotic manta proposed in this paper is mainly propelled by vertical waves generated by flapping fins on both sides. For the crank rocker mechanism, it is important to determine the mapping relationship between the rotational motion of the drive rod *b* and the vertical displacement of the two sets of output rods. Therefore, the movement experiment of the left pectoral fin of robotic manta is carried out under the SolidWorks simulation environment. When a constant angular velocity ($\omega = 2\pi$ rad/s) is given to rod *b* (assuming counterclockwise is positive), the vertical displacement relationship between the four key points of two rod groups (as shown in Fig. 3) is shown in Fig. 10. As can be seen from the curves, the four key points of the output rods move approximately sinusoidally in the vertical direction.

It can be seen from Fig. 10 (a) that in linkage group I, the end motion of the short rod *f* is ahead of the end of the long rod *i*, which confirms the assumption in Fig. 4 (a). Moreover, the difference between the starting points of the upstroke of the two rods is about 0.25T, which is consistent with biological studies. The swing amplitude of the short rod *f* can reach 46.01 mm while the swing amplitude of long rod *i* reaches 258.96 mm.

Fig. 10 (b) shows that the bevel gear mechanism effectively changes the motion phase of two sets of output rods. In addition, by adjusting the gear tooth coupling, when the difference between the initial angles of b_1 and b_2 is 30°, point A leads point C by 1/12T.

Fig. 10 (c) shows that although the swing amplitude of the two long rods is different, the phase difference is almost 1/12T, which proves the effectiveness of the previous design.

Since the pectoral fins on both sides adopt symmetrical structure, the rotation angle of the rod *b* is further described as follows:

$$\begin{cases} \theta_L(t) = \int_0^t \omega_L(t)dt + \theta_{L0} \\ \theta_R(t) = \int_0^t \omega_R(t)dt + \theta_{R0} \end{cases} \tag{4}$$

Among them, $\theta_L(t)$ and $\theta_R(t)$ represent the rotation angle of b_1 and b_2 with respect to the bracket *a* at the moment *t*. θ_{L0} and θ_{R0} represent the initial bias angle of b_1 and b_2 relative to bracket *a* respectively. $\omega_L(t)$ and $\omega_R(t)$ represent the angular velocities of b_1 and b_2 at moment *t*.

When the initial offset angle and angular velocity change, the robotic manta can achieve several different swimming modes. Note that the horizontal swing angle ψ of both sides should be symmetrical and equal.

The forward swimming mode is most commonly used in underwater vehicles equipped with wave fins [16]. When the constant angular velocity of both sides is symmetrical and the initial offset angle equals, the spanwise propulsion forces generated by the pectoral fins cancel each other out, and the propulsive force along stream wise will push the robotic manta forward to realize the forward swimming mode. The kinematic relationship can be described as

$$\begin{cases} \omega_L(t) = \omega(t) \\ \omega_R(t) = -\omega(t) \\ \theta_{L0} = \theta_{R0} \end{cases} \tag{5}$$

Manta rays are known for their high maneuverability. The robotic manta presented in this paper can also achieve turning movement with the cooperation of the pectoral fins. When one side of the pectoral fin remains relatively stationary and the other side is given a fixed angular velocity, the thrust on the stationary side disappears and the turning movement can be achieved. Kinematically, it follows that

$$\begin{cases} \omega_L(t) = \omega(t) \\ \omega_R(t) = 0 \end{cases} \tag{6}$$

Or

$$\begin{cases} \omega_L(t) = 0 \\ \omega_R(t) = -\omega(t) \end{cases} \tag{7}$$

In addition, the robotic manta can adjust their pitching posture to realize 3D movement with the aid of buoyancy adjustment mechanism and caudal fin. When the buoyancy adjustment mechanism inhales a certain amount of water, the centroid of the robotic manta moves forward, and its buoyancy is reduced, so that the diving mode can be achieved. On the

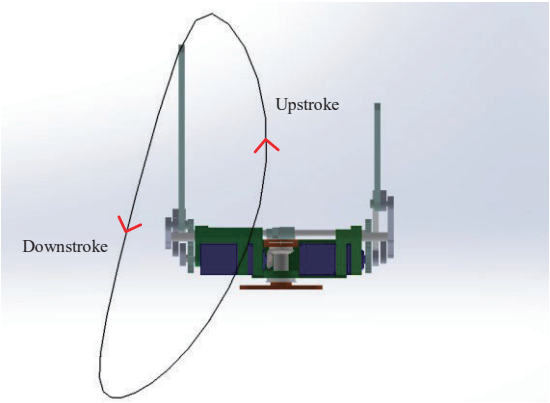

Fig. 11. Simulation of the tip trajectory.

contrary, when the buoyancy adjustment mechanism discharges some water, the floating mode can be realized

B. Compound Motion

As previously mentioned, the highly efficient swimming of manta rays is closely related to the tip trajectory of their pectoral fins. Based on the basic swimming mode, with the bevel gear mechanism, the pectoral fins can realize compound motion which contributes to tracking the tip trajectory. ψ represents the angle at which the midline of the pectoral fin turns relative to the rotation center. For simplicity, denote ψ of both sides as ψ_L and ψ_R, respectively. Moreover, suppose the fins swing sinusoidally in horizontal plane. That is, the following relationship maintains

$$\begin{cases} \psi_L = \psi_M \sin\left(2\pi ft + \psi_{L0}\right) \\ \psi_R = \psi_M \sin\left(2\pi ft + \psi_{R0}\right) \end{cases} \tag{8}$$

where, ψ_M represents the maximum swing amplitude. ψ_{L0} and ψ_{R0} represent the initial phase angle, and f represents the frequency of sinusoidal motion.

Then, the simulation of tip trajectory tracking is carried out under the SolidWorks environment. In forward swimming mode, we provide $\psi_{L0} = \psi_{R0} = 0°$ and $f = 1$ Hz and $\psi_M = 20°$. Fig. 11 shows the simulation trajectory. As can be easily identified, the built robotic manta is able to track the approximate tip trajectory given in Fig. 7 (a). It is worth noting that the simulation trajectory and the reference trajectory are not identical. However, this similarity indicates that the tip of robotic pectoral fin has the ability of complex 3D movement, which can meet the control requirements.

IV. Conclusions and Future Work

In this paper, based on improved crank rocker mechanism, we have developed a novel bionic robot manta with unique pectoral fins which can generate two propulsive waves vertical to each other. According to the detailed analysis of the crank rocker mechanism, the geometrical parameters of the pectoral fin is determined. On this basis, a horizontal DOF is added to the pectoral fin to track the tip trajectory of real pectoral fins. These two key features make the robotic manta expected to swim efficiently and fast. In addition, considering the wide profile of the robotic manta, we design a new type of buoyancy adjustment mechanism to acquire 3D motion and gliding abilities. Specifically, simulation analyses verify the feasibility of the theoretical design. Finally, basic control strategies and tip trajectory tracking method are presented. It should be remarked that the current work only provides a preliminary result.

The ongoing and future work will concentrate on dynamic modeling and aquatic experiments. Besides, the robotic manta will be equipped with a ZED camera and a high-performance processor, which is expected to be exploited as a mobile platform for underwater applications in the future.

References

[1] M. Sfakiotakis, D. M. Lane, and J. B. C. Davies, "Review of fish swimming modes for aquatic locomotion," *IEEE J. Ocean. Eng.*, vol. 24, no. 2, pp. 237–252, Apr. 1999.

[2] M. S. Triantafyllou and G. S. Triantafyllou, "An efficient swimming machine," *Scientific American*, vol. 272, no. 3, pp. 40–48, 1995.

[3] Z. Wu, J. Yu, J. Yuan, M. Tan, and J. Zhang, "Mechatronic design and implementation of a novel gliding robotic dolphin," in *Proc. IEEE Int. Conf. Robot. Biomim.*, Zhuhai, China, Dec. 2015, pp. 267–272.

[4] J. Liang, T. Wang, and L. Wen, "Development of a two-joint robotic fish for real-world exploration," *J. Field Robot*, vol. 28, no. 1, pp. 70–79, 2011.

[5] Z. Wang, Y. Wang, J. Li, and G. Hang, "A micro biomimetic manta ray robot fish actuated by SMA," *in Proc. IEEE Int. Conf. Robot. Biomim.*, Guilin, China, pp. 1809–1813, 2009.

[6] F. E. Fish, C. M. Schreiber, K. W. Moored, G. Liu, H. Dong, and H. Bart-Smith, "Hydrodynamic performance of aquatic flapping: efficiency of underwater flight in the manta," *Aerospace*, vol. 3, no. 3, p. 20, 2016.

[7] C. Chew, Q. Lim, and K. S. Yeo, "Development of propulsion mechanism for Robot Manta Ray," in *Proc. IEEE Int. Conf. Robot. Biomim.*, Zhuhai, China, Dec. 2015, pp. 1918–1923.

[8] K. H. Low, C. Zhou, G. Seet, S. Bi, and Y. Cai, "Improvement and testing of a robotic manta ray (RoMan-III)," in *Proc. IEEE Int. Conf. Robot. Biomim.*, Karon Beach, Phuket, 2011, pp. 1730–1735.

[9] R. S. Russo, S. S. Blemker, F. E. Fish, and H. Bart-Smith, "Biomechanical model of batoid (skates and rays) pectoral fins predicts the influence of skeletal structure on fin kinematics: implications for bio-inspired design," *Bioinspir. Biomim.*, vol. 10, no. 4, p. 046002, 2015.

[10] J. E. Fontanella, F. E. Fish, E. I. Barchi, R. Campbell-Malone, R. H. Nichols, N. K. DiNenno, J. T. Beneski, "Two-and three-dimensional geometries of batoids in relation to locomotor mode," *J. Exp. Marine Biol. Ecology*, vol. 446, pp. 273–281, 2013.

[11] D. C. Webb, P. J. Simonetti, and C. P. Jones, "SLOCUM: an underwater glider propelled by environmental energy," *IEEE J. Ocean. Eng.*, vol. 26, no. 4, pp. 447–452, 2001.

[12] C. C. Eriksen, T. J. Osse, R. D. Light, T. Wen, T. W. Lehman, P. L. Sabin, J. W. Ballard, A. M. Chiodi, "Seaglider: A long-range autonomous underwater vehicle for oceanographic research," *IEEE J. Ocean. Eng.*, vol. 26, no. 4, pp. 424–436, 2001.

[13] J. Sherman, R. E. Davis, W. B. Owens, and J. Valdes, "The autonomous underwater glider 'Spray'," *IEEE J. Ocean. Eng.*, vol. 26, no. 4, pp. 437–446, 2001.

[14] G. Liu, Y. Ren, J. Zhu, H. Bart-Smith, H. Dong, "Thrust producing mechanisms in ray-inspired underwater vehicle propulsion," *Theor. Appl. Mech. Lett.*, vol. 5, no. 1, pp. 54–57, 2015.

[15] G. Li, Y. Deng, O. L. Osen, S. Bi, and H. Zhang, "A bio-inspired swimming robot for marine aquaculture applications: From concept design to simulation," in *OCEANS 2016 - Shanghai*, April 2016, pp. 1–7.

[16] M. Sfakiotakis, D.M. Lane, and J. B. C. Davies, "Review of fish swimming modes for aquatic locomotion," *IEEE J. Ocean. Eng.*, vol. 24, no. 2, pp. 237–252, Apr. 1999.